

Observations of Neutral Atoms from the Solar Wind

Michael R. Collier¹, Thomas E. Moore¹, Keith W. Ogilvie¹,
Dennis Chornay^{1,2}, J.W. Keller¹, S. Boardsen¹, James Burch³,
B. El Marji^{1,2}, M.-C. Fok¹, S.A. Fuselier⁴, A.G. Ghielmetti⁴, B.L. Giles¹,
D.C. Hamilton², B. Peko⁵, J.M. Quinn⁶, T. Stephen⁵, G.R. Wilson⁷ and P. Wurz⁸

1. NASA/Goddard Space Flight Center, Greenbelt, Maryland

2. University of Maryland, College Park

3. Southwest Research Institute, San Antonio, Texas

4. Lockheed Martin Advanced Technology Center, Palo Alto, California

5. Denver University, Colorado

6. University of New Hampshire, Durham

7. Mission Research Corporation, Nashua, New Hampshire

8. University of Bern, Switzerland

date: 14 September 2000 – version: 3.0

Abstract. We report observations of neutral atoms from the solar wind in the Earth’s vicinity with the Low Energy Neutral Atom (LENA) imager on the IMAGE spacecraft. This instrument was purposely designed to be capable of looking at and in the direction of the Sun. Observed enhancements in the hydrogen count rate in the solar direction are correlated with neither solar ultraviolet emission nor suprathermal particles and are therefore deduced to be due to neutral particles from the solar wind. Based on the presence of oxygen, presumably sputtered from the conversion surface, observed in the time-of-flight (tof) spectra, the energy of these neutral particles exceeds ~ 1 keV, consistent with solar wind energies. In addition, the sputtered oxygen abundance tracks the solar wind speed, even when IMAGE is deep inside the magnetosphere. These results show that low energy neutral atom imaging provides the capability to directly monitor the solar wind and/or magnetosheath from inside the magnetosphere.

1. Introduction

The Low Energy Neutral Atom (LENA) imager, one of six science experiments launched on the IMAGE observatory on March 25, 2000, was designed for remote sensing of the neutral component of space plasmas at energies from a few tens to a few thousands of electron volts [Moore *et al.*, 2000]. Neutral particles in this energy where much, if not most, of the plasma in the heliosphere resides, have not previously been systematically observed. Like instruments which image more energetic neutral atoms, LENA has the ability not only to detect neutral atoms, but also to determine their direction polar and azimuthal angles as well as their mass and energy [Hsieh *et al.*, 1992]. Because LENA was specifically designed to observe the sun directly and responds to neutrals of energies of the order of 1 keV, the instrument is capable of observing that fraction of the solar wind flow that is neutral hydrogen, which has been long-recognized as of potentially great importance for understanding solar, interplanetary and magnetospheric physics [Akasofu, 1964; Wurz *et al.*, 1995].

Charge exchange between solar wind protons and neutral particles can be primarily responsible for the formation of a neutral solar wind, although there is a neutral component of the solar wind due to recombination of solar wind ions with solar wind electrons [Gruntman, 1994]. The neutrals with which the solar wind protons charge exchange may be interstellar neutral atoms, originate from dust grains [Holzer, 1977; Schwadron *et al.*, 2000] or be part of the Earth's geocorona. To highlight the potential importance of charge exchange with the Earth's exosphere, note that the geocoronal density at the magnetopause is comparable to the solar wind density [Rairden *et al.*, 1986]. Also because charge exchange with the geocorona will occur preferentially near the Earth, the neutral solar wind characteristics may

be heavily influenced by magnetospheric structures such as the magnetopause and cusp and activity of the magnetosphere. This will lead to wider angular profiles with signals coming from directions offset from what might be expected from solar wind charge exchange upstream of the Earth's bowshock. In addition, if the Earth is in conjunction with Venus, LENA might observe an increased neutral solar wind flux due to charge exchange in the Venus atmosphere.

2. Observations from the June 8, 2000 Event

After beginning science operations on May 5, 2000, LENA had an opportunity about a month later to observe a coronal mass ejection (CME) and its effect on the terrestrial environment (see companion papers in this issue by Moore *et al.* [2000] and Fuselier *et al.* [2000]). On June 6, 2000, an intense solar flare was observed on the sun followed by a full-halo CME propagating toward the Earth. The shock driven by this CME was observed on June 8, 2000 at the L1 point, 235 R_E upstream from the Earth, by the ACE and SOHO spacecraft at about 08:42 UT and by the Wind spacecraft, 41 R_E upstream, at about 09:05 UT. At 09:11 UT this disturbance passed the Earth where it and its effects were observed by the IMAGE spacecraft.

Figure 1 shows a LENA spectrogram of the combined hydrogen and oxygen count rate as a function of time on June 8, 2000, the day the CME-driven shock passed the Earth. Also see the first two panels of Figure 4 of Moore *et al.* [2000] for an image of the sun pulse brightening. The bright streak hovering near 180° is a signal initially thought to represent a response to the EUV photon flux from the Sun. The angular range of the Earth is indicated by the dashed white lines, and the yellow brightening around 09:50 UT is the oxygen burst discussed by Fuselier *et al.* [2000]. However, when the sun pulse signal increased significantly at the arrival of

a shock (at 09:11 UT) in the solar wind associated with a CME, it was concluded that at least part of this signal must represent neutral atoms from the solar wind. Subsequent analysis based on in-flight and calibration data show LENA to have a negligible response to UV at ambient pressures experienced on orbit.

As additional evidence that LENA is not responding to UV, Figure 2 shows the EUV data from the Solar and Heliospheric Observatory on June 6-8, 2000 [*Judge et al.*, 1998]. The upper solid line shows the photon flux between 0.1 and 50 nm and the lower dashed curve shows the photon flux between 24 and 34 nm. The activity on June 6 associated with the CME is apparent in the data with some subsequent activity on June 7 (which was not associated with a LENA count rate enhancement). During the event on June 8, indicated by the vertical line, there is no enhancement in the UV flux, indicating that LENA is not responding to photons.

Given that UV is not the cause of the observed enhancement from the solar direction, one must examine the possibility that this increase is due to suprathermal ions penetrating the collimator [*Moore et al.*, 2000]. At the time of the June 8, 2000 event a potential about 8.8 kV was across the collimator, filtering out all particles with energies up to 55 keV/e while above about 83 keV/e most ions traverse the collimator and arrive inside the instrument. The gap between the collimator plates varies from about 20 mm at the front to about 12 mm at the back so that the electric field varies from 444 to 730 kV/m over a distance of 93 mm. Because energetic ion spectra at these energies in most space plasma environments are rapidly decreasing power laws [*Collier et al.*, 1993], the primary contributor to the energetic ion flux entering LENA in-flight is likely close to the 55 keV/e lower limit on entering ion energy.

In Figure 3, the left hand y-axis corresponds to the solid lines and circles and

shows the time profile of the LENA background-adjusted Sun direction counts per spin. The profile peaks shortly after shock passage and slowly drops for about an hour thereafter. The ACE/EPAM ion flux data between 47 and 65 keV, which includes the 55 keV low energy limit on LENA ion admittance, show on this day practically a step function increase by a factor of 25-50 at the time of the shock. If LENA were responding to energetic ions, therefore we would expect the time profile for the two rates to be more similar. This suggests that LENA is not responding to suprathermal particles at this time.

Further evidence of this is given in Fig. 3 which shows the solar wind ram pressure observed by the Wind spacecraft (with dashed lines on the right hand y-axis). The times when the high latitude magnetopause model of Boardsen *et al.* [2000] predicts that IMAGE is inside the magnetosphere are indicated by the black bars on the top x-axis. The Wind spacecraft at this time was about 41 R_E upstream and about 27 R_E off the Sun-Earth line in the minus y GSE direction, well within the $\sim 40 R_E$ scale length inferred by Collier *et al.* [1998] for IMF correlations making it likely that Wind was a reliable interplanetary monitor. Although the Boardsen *et al.* model predicts that IMAGE moved across the magnetopause eight times in this three hour period, there are no sudden jumps in the LENA count rate associated with these crossings similar to what would be expected in ion data at energies around 80 keV. Furthermore, when IMAGE is inside the magnetosphere, we would not expect the energetic particles to arrive from a narrow range of directions as the “sun pulse” does.

By eliminating UV light and charged particles as possible sources, we conclude LENA to be observing neutral particles from the solar direction at this time, indicating the sun pulse in general to be overwhelmingly due to neutral particles. We

now address the issue of whether or not the neutral atom energy is consistent with solar wind-like energies of the order of 1-5 keV. Figure 4 shows LENA calibration data taken at the Denver University neutral beam facility [*Stephen et al.*, 1996]. The upper panel shows a time-of-flight spectrum resulting from incident 30 eV atomic hydrogen. There is a well-defined hydrogen peak at low times-of-flight with no evidence of an oxygen peak. An oxygen peak appears when the energy of the incident neutral hydrogen falls between 300 eV and 1000 eV. Above this transition, as shown in the lower panel of Fig. 4 for 1000 eV atomic hydrogen, a significant oxygen peak is present, believed to be due to high energy hydrogen sputtering of adsorbed oxygen or water from the conversion surface.

Figure 5 shows a time-of-flight spectrum taken over the time period of the enhancement on June 8, 2000. In addition to the hydrogen and oxygen peaks, there is a third peak which appears in the in-flight data but not in the calibration data probably because in-flight the instrument is running at a higher start microchannel plate bias level. Note that there is a pronounced oxygen peak in the time-of-flight spectrum. Since large neutral oxygen fluxes do not occur in the solar wind, this suggests the neutral hydrogen has energy ~ 1 keV, above which sputtering can occur.

However, there is a relatively larger oxygen signal in Fig. 5, the in-flight data, as compared to Fig. 4, the calibration data. Because LENA was only calibrated to 1 keV at which energy the sputtered oxygen appears, we cannot make any quantitative statements about the energy of the neutral hydrogen except that it is comparable to or greater than 1 keV. It is possible that this relative abundance is a very sensitive function of energy which might explain the larger relative abundance of oxygen to hydrogen in the in-flight data. In addition, it is possible that at higher energies part of the hydrogen peak is also of sputtered origin.

The ratio of hydrogen to oxygen in the LENA time-of-flight spectrum may be used to monitor solar wind speed from inside the magnetosphere. The left hand y-axis and solid line in Figure 6 show, as a function of time, the solar wind speed as observed by the SWE instrument on Wind. The right hand y-axis and solid circles indicate the background-adjusted integrated hydrogen to oxygen count ratio in the sun sector from hourly averaged tof spectra. Prior to the shock passage, the ratio is 0.29 while after the shock passage the ratio is 0.46 indicating that LENA has observed the solar wind speed increase from inside the magnetosphere.

3. Discussion

Having argued that LENA has observed neutral particles from the solar wind, we now estimate the neutral flux during the enhancement period and compare to expectations. Based on Fig. 3, the count rate during the enhancement is about 15 counts per spin. Each spin sector is observed for about 2.7 seconds so that this is a count rate of 5.6 s^{-1} . At solar wind energies, LENA's neutral hydrogen efficiency was measured to be about 6.4×10^{-5} . We regard this as being correct to within a factor of two. With LENA's 1 cm^2 aperture, this implies a flux of about $8.8 \times 10^4 \text{ cm}^{-2} \text{ s}^{-1}$. At this time, the solar wind flux was $\sim 10^9 \text{ cm}^{-2} \text{ s}^{-1}$ (12 cm^{-3} density and 800 km/s speed) yielding a flux ratio of neutrals to solar wind protons of about 10^{-4} .

This value is comparable to the expected neutral solar wind component at 1 AU [*Holzer, 1977; Gruntman, 1994*]. However, the LENA observations include a potentially significant contribution due to charge exchange with the geocorona which might raise the ratio significantly. On the other hand, given the IMAGE orbit on June 8, 2000, the neutral solar wind impinges on LENA close to the edge

of its field-of-view and so may be incompletely observed.

To illustrate the potential importance of charge exchange with the Earth's geocorona, we will show a simple estimate of the expected fraction of the flux signal resulting from this effect. The hydrogen atom distribution in the geocorona is a smoothly varying function of the distance from the center of the planet. Using the geocoronal density $N(R)$ determined by Wallace *et al.* [1970] as

$$N(R) = 10 \cdot \left(\frac{11}{R}\right)^3 \text{ cm}^{-3}, \quad (1)$$

where R is the distance from the Earth in Earth radii, we can calculate the neutral atom flux due to charge exchange with the geocorona F_{ce} . The range of Wallace *et al.*'s data is about 3-15 R_E . Following the work of Roelof [1997] and Roelof and Skinner [2000] we write

$$F_{ce} = \int_{r_{mp}}^{\infty} N(R) \sigma n_{sw} v_{sw} dR, \quad (2)$$

where r_{mp} is the distance of the magnetopause from the Earth.

The solar wind neutrals are expected to emerge from the charge exchange collision with their initial velocity, v_{sw} , and the solar wind density, n_{sw} , not significantly depleted so that the fraction of the solar wind density we expect to be neutral due to its interaction with the Earth's geocorona is simply

$$\frac{n_{ce}}{n_{sw}} = \int_{r_{mp}}^{\infty} N(R) \sigma dR, \quad (3)$$

Using equation (1) for the neutral density and taking $\sigma = 2 \times 10^{-15} \text{ cm}^2$, we get

$$\begin{aligned} \frac{n_{ce}}{n_{sw}} &= 10 \text{ cm}^{-3} \cdot 11^3 \cdot 2 \times 10^{-15} \text{ cm}^2 \cdot 6371 \times 10^5 \text{ cm} \cdot \int_{r_{mp}}^{\infty} \frac{dR}{R^3} \\ &= \frac{8.5 \times 10^{-3}}{r_{mp}^2}, \end{aligned} \quad (4)$$

where r_{mp} is measured in Earth radii.

At standard magnetopause distances of $10 R_E$, this results in a fraction of about 10^{-4} , comparable to the expected neutral solar wind component at 1 AU [*Holzer, 1977; Gruntman, 1994*] so that this effect under normal circumstances will tend to double the neutral solar wind flux.

9. Conclusions

We have reported observations of a count rate increase observed by the LENA imager on June 8, 2000 when a shock driven by a CME associated with a solar flare on June 6, 2000 arrived at the Earth. By establishing that the signal coming from the general direction of the sun is neither due to UV photons nor due to suprathermal particles, we have concluded that the enhancement and likely the pre- and post-event signal are due to neutrals in the solar wind. We have shown based on a comparison between LENA time-of-flight spectra from calibration and from this event that the observed neutral hydrogen energies are ~ 1 keV, energies characteristic of the solar wind. In addition, we observed in the solar wind neutral particles the large solar wind velocity jump associated with the shock passage. We estimate based on LENA efficiencies from calibration data the observed neutral solar wind flux, and we arrive at a solar wind neutral flux to solar wind ion flux ratio of about 10^{-4} , consistent with expected neutral solar wind fluxes at 1 AU. However, we point out that much of this signal may be due to solar wind charge exchange with the geocorona near the magnetopause. These results show that low energy neutral atom imaging may provide the capability to directly monitor the solar wind and/or magnetosheath from inside the magnetosphere.

Acknowledgments. This research supported by the Explorer Program at NASA's GSFC under Mission Operations and Data Analysis UPN 370-28-20. Michael R. Collier's involvement with the LENA instrument began while he was a National Research Council Resident Research Associate in the Electrodynamics Branch, Code 696. Thanks to Professor Darrel Judge, USC, CA for SOHO/SEM data.

References

- Akasofu, S.-I., The neutral hydrogen flux in the solar plasma flow - I, *Planet. Space Sci.*, *12*, 905-913, 1964.
- Boardsen, S.A., T.E. Eastman, T. Sotirelis and J.L. Green, An empirical model of the high-latitude magnetopause, *J. Geophys. Res.*, in press, 2000.
- Collier, Michael R., On generating kappa-like distribution functions using velocity space Lévy flights, *Geophys. Res. Lett.*, *20*, 1531-1534, 1993.
- Collier, Michael R., J.A. Slavin, R.P. Lepping, A. Szabo and K. Ogilvie, Timing accuracy for the simple planar propagation of magnetic field structures in the solar wind, *Geophys. Res. Lett.*, *25*, 2509-2512, 1998.
- Fuselier, S.A., A.G. Ghielmetti, T.E. Moore, M.R. Collier, J.M. Quinn, G.R. Wilson, P. Wurz, S.B. Mende, H.U. Frey, C. Jamar, J.-C. Gerard and J.L. Burch, Ion outflow observed by IMAGE: Implications for source regions and heating mechanisms, *Geophys. Res. Lett.*, submitted, 2000.
- Gruntman, Michael A., Neutral solar wind properties: Advance warning of major geomagnetic storms, *J. Geophys. Res.*, *99*, 19,213-19,227, 1994.
- Holzer, Thomas E., Neutral hydrogen in interplanetary space, *Rev. Geophys. and Space Phys.*, *15*, 467-490, 1977.
- Hsieh, K.C., C.C. Curtis, C.Y. Fan and M.A. Gruntman, Techniques for the remote sensing of space plasma in the heliosphere via energetic neutral atoms: A review, Solar Wind Seven (Proceedings of the Third COSPAR Symposium), E. Marsch and R. Schwenn, eds., Pergamon, New York, 357-364, 1992.
- Judge, D.L., D.R. McMullin, H.S. Ogawa, D. Hovestadt, B. Klecker, M. Hilchenbach, E. Möbius, L.R. Canfield, R.E. Vest, R. Watts, C. Tarrio, M. Kühne and P. Wurz, First solar EUV irradiances obtained from SOHO by the

CELIAS/SEM, *Solar Physics*, 177, 161-173, 1998.

Moore, T.E., D.J. Chornay, M.R. Collier, F.A. Herrero, J. Johnson, M.A. Johnson, J.W. Keller, J.F. Laudadio, J.F. Lobell, K.W. Ogilvie, P. Rozmarynowski, S.A. Fuselier, A.G. Ghielmetti, E. Hertzberg, D.C. Hamilton, R. Lundgren, P. Wilson, P. Walpole, T.M. Stephen, B.L. Peko, B. Van Zyl, P. Wurz, J.M. Quinn and G.R. Wilson, The Low-Energy Neutral Atom Imager for IMAGE, *Space Sci. Rev.*, 91, 155-195, 2000.

Moore, T.E., M.R. Collier, J.L. Burch, D.J. Chornay, B. El Marji, S.A. Fuselier, A.G. Ghielmetti, B.L. Giles, D.C. Hamilton, F.A. Herrero, J.W. Keller, K.W. Ogilvie, B.L. Peko, J.M. Quinn, T.M. Stephen, G.R. Wilson and P. Wurz, Low energy neutral atoms in the magnetosphere, *Geophys. Res. Lett.*, submitted, 2000.

Rairden, R.L., L.A. Frank and J.D. Craven, Geocoronal imaging with Dynamics Explorer, *J. Geophys. Res.*, 91, 13,613-13,630, 1986.

Roelof, E.C., Energetic neutral atom imaging of magnetospheric ions from high and low-altitude spacecraft, *Adv. Space Res.*, 20, 341-350, 1997.

Roelof, Edmond C. and Andrew J. Skinner, Extraction of ion distributions from magnetospheric ENA and EUV images, *Space Sci. Rev.*, 91, 437-459, 2000.

Schwadron, N.A., J. Geiss, L.A. Fisk, G. Gloeckler, T.H. Zurbuchen and R. von Steiger, Inner source distributions: Theoretical interpretation, implications, and evidence for inner source protons, *J. Geophys. Res.*, 105, 7465-7472, 2000.

Stephen, T.M., B. Van Zyl and R.C. Amme, Generation of a fast atomic-oxygen beam from O^- ions by resonant cavity radiation, *Rev. Sci. Instrum.*, 67, 1478-1482, 1996.

Wallace, L., Charles A. Barth, Jeffrey B. Pearce, Kenneth K. Kelly, Donald E.

- Anderson, Jr. and William G. Fastie, Mariner 5 measurement of the Earth's Lyman alpha emission, *J. Geophys. Res., Space Physics*, *75*, 3769-3777, 1970.
- Wurz, P., M.R. Aellig, P. Bochsler, A.G. Ghielmetti, E.G. Shelly, S. Fuselier, F. Herrero, M.F. Smith and T. Stephen, Neutral atom imaging mass spectrograph, *Opt. Eng.*, *34*, 2365-2376, 1995.

Figure Captions

Figure 1. A LENA spectrogram showing the combined hydrogen and oxygen count rate as a function of time on June 8, 2000. The y-axis shows the spacecraft spin angle. The direction and angular range of the Earth is indicated by the white dashed lines. The “sun pulse” is the streak hovering around 180° . This signal increases by about a factor of two when the shock passes at 09:11 UT.

Figure 2. EUV data showing photon flux from SOHO on June 6-8, 2000. The upper solid line is the photon flux from 0.1-50 nm and the lower dashed curve shows the photon flux from 24-34 nm. The flares on June 6 and 7 are apparent in the data. However, there is no enhancement during the event on June 8, showing that LENA is not responding to UV light at this time.

Figure 3. A comparison between the LENA sun sector count rate data and the solar wind ram pressure on June 8, 2000. This figure also shows with black bars along the upper x-axis when the IMAGE spacecraft based on the high-latitude magnetopause model of Boardsen *et al.* [2000] is inside the magnetosphere. The model predicts that during the June 8, 2000 event IMAGE moved back and forth across the magnetopause many times. This implies that if IMAGE were responding to energetic particles during this time, there would be changes in the signal corresponding to the boundary crossings. Because no such changes are observed and the distribution is less isotropic than would be expected from energetic particles, it is concluded that LENA is not responding to suprathermal ions during this time period. Both the solar wind ram pressure and the Boardsen *et al.* model results are derived from Wind spacecraft data.

Figure 4. The two panels in this figure show a comparison of the time-of-flight

spectra from the Denver University calibration resulting from incident atomic hydrogen. The top panel shows a time-of-flight spectrum resulting from 30 eV atomic hydrogen. Note the absence of a sputtered oxygen peak. The lower panel shows a time-of-flight spectrum resulting from 1 keV atomic hydrogen. At this higher, solar wind energy, a sputtered oxygen peak is apparent in the time-of-flight data.

Figure 5. This figure shows a LENA time-of-flight spectrum taken during the June 8, 2000 event from 0900-1100 UT. The spectrum only includes events coming from the general direction of the sun. The pronounced oxygen peak in the spectrum indicates that the neutral hydrogen energies are ~ 1 keV, consistent with expected neutral solar wind energies.

Figure 6. The jump in solar wind speed observed by Wind during the shock passage on June 8, 2000, indicated by the solid line and left hand y-axis, is reflected in the ratio of atomic hydrogen to sputtered oxygen signal observed by LENA coming from the direction of the sun, indicated by the solid circles and right hand y-axis. The data in this figure are integrated counts from the sun direction over all spins during the one hour intervals. The hydrogen peak was taken to be channels 151-190 and the oxygen peak was taken to be channels 401-1000. A background rate was subtracted off both the hydrogen and oxygen peaks based on the number of counts appearing between channels 301-400, where no peak is expected. The count rates during this period are low enough so that the microchannel plates are not saturating. Because IMAGE is inside the magnetosphere during most of the time period covered by Fig. 6, these results indicate that low energy neutral atom imagers can directly monitor interplanetary conditions from inside the magnetosphere.

IMAGE/LENA

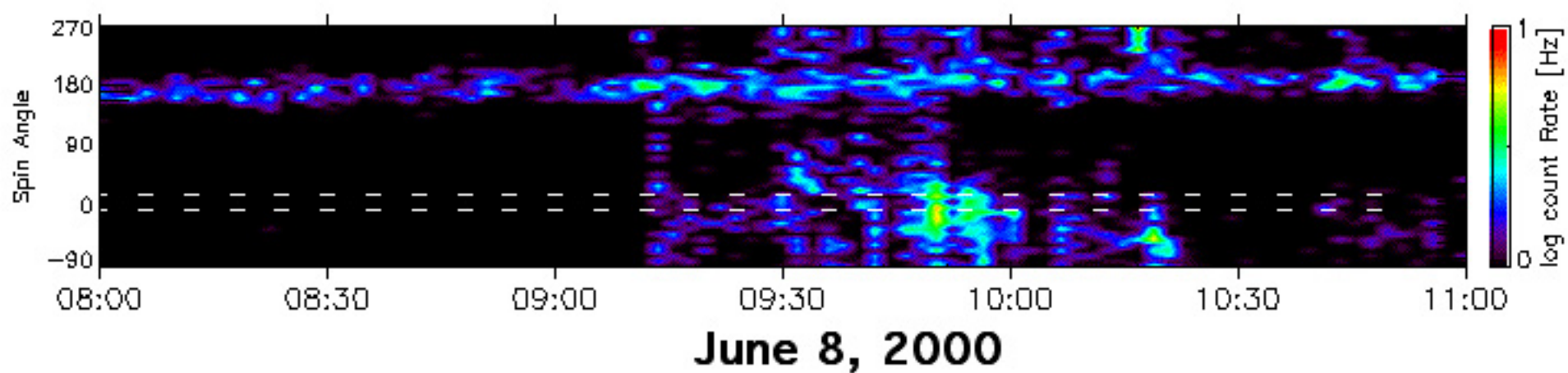


figure 1

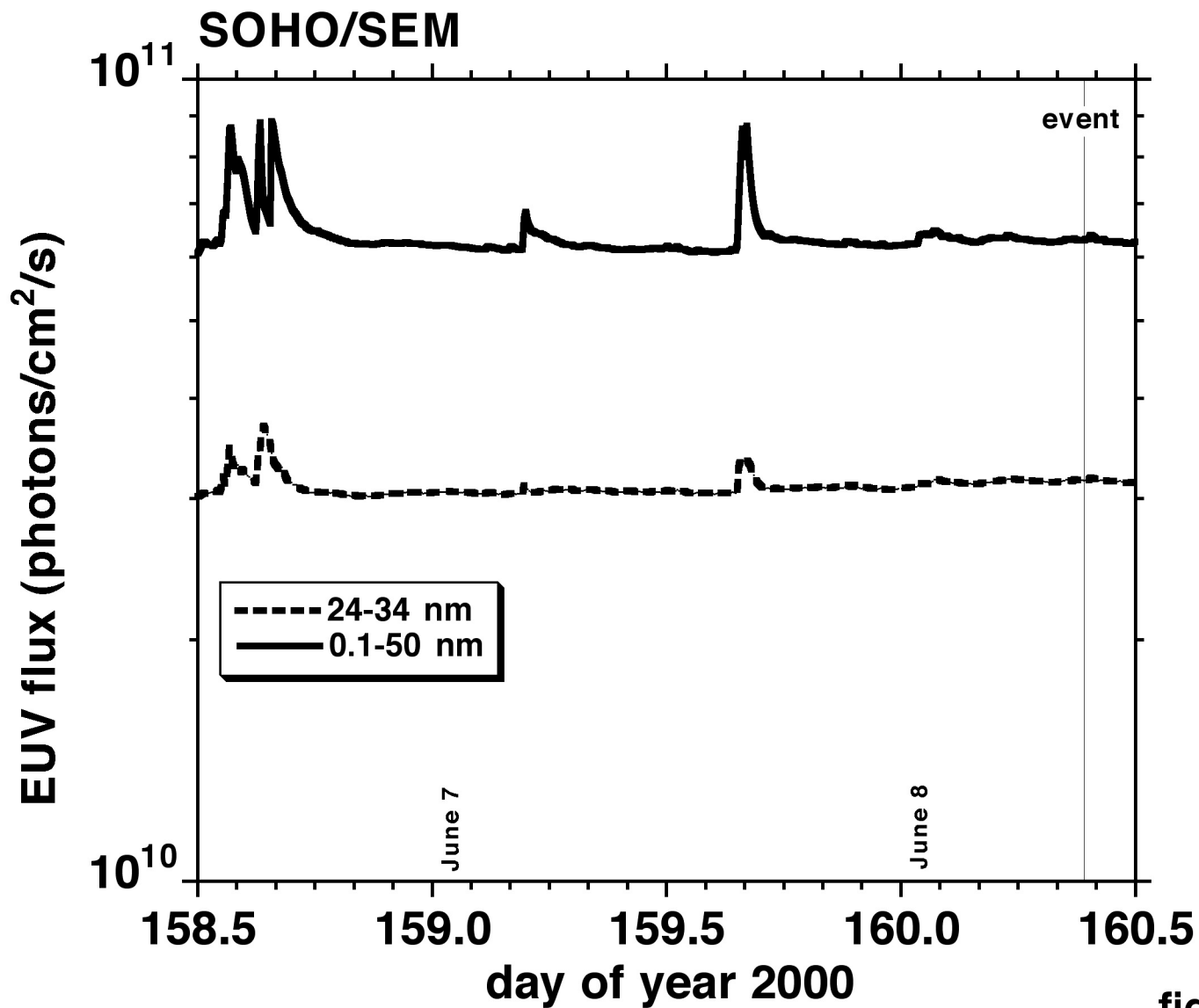


figure 2

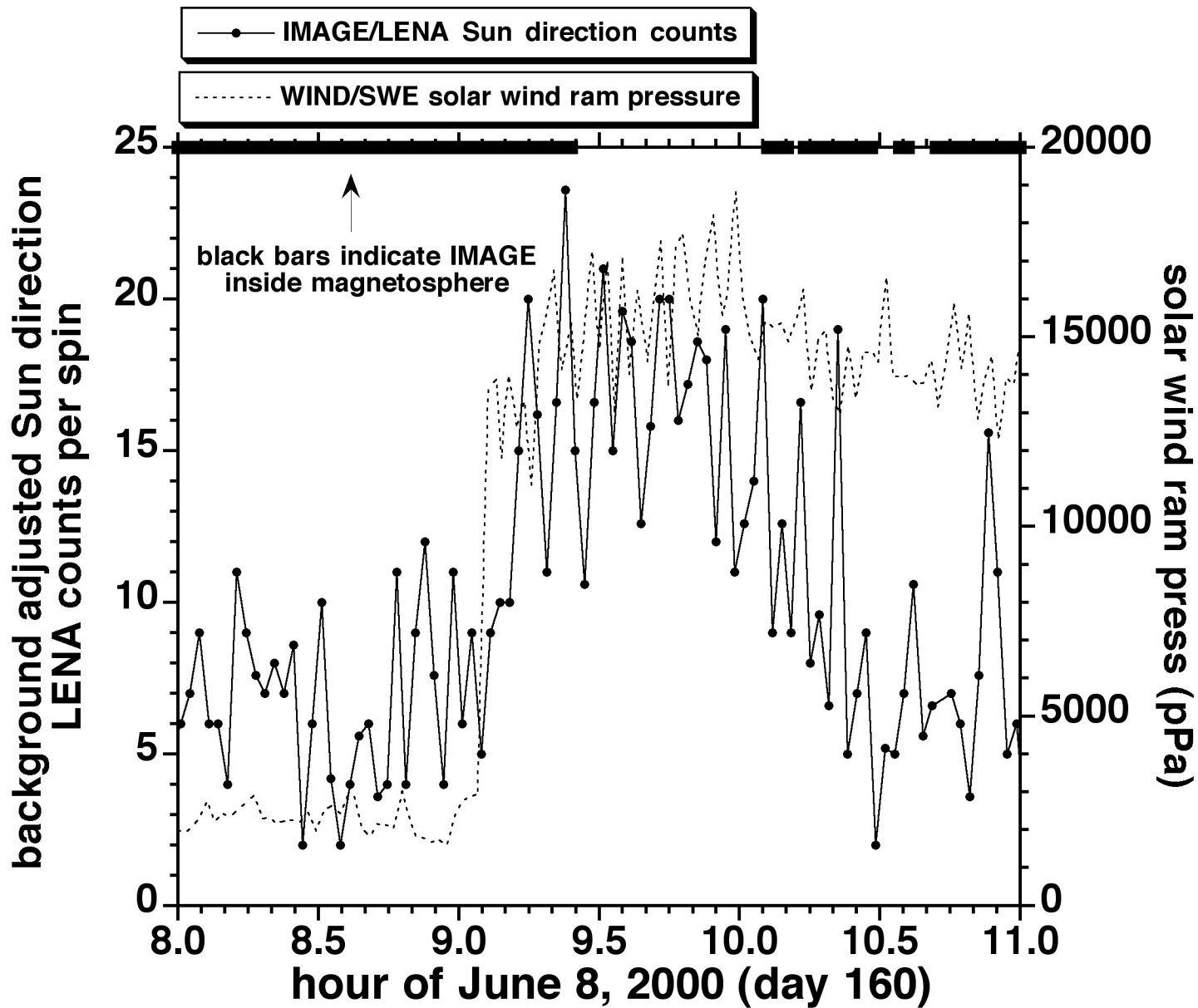


figure 3

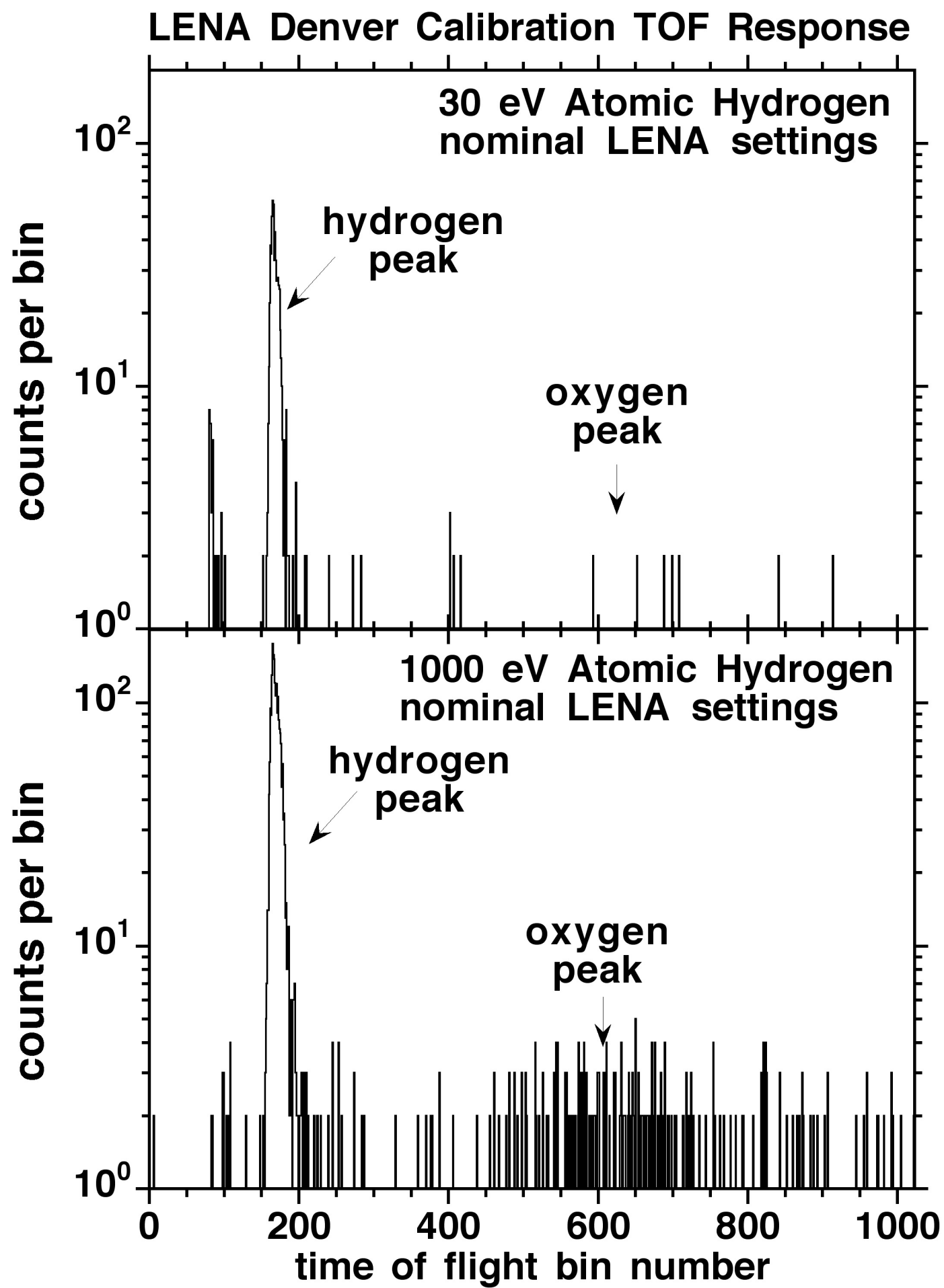


figure 4

IMAGE/LENA

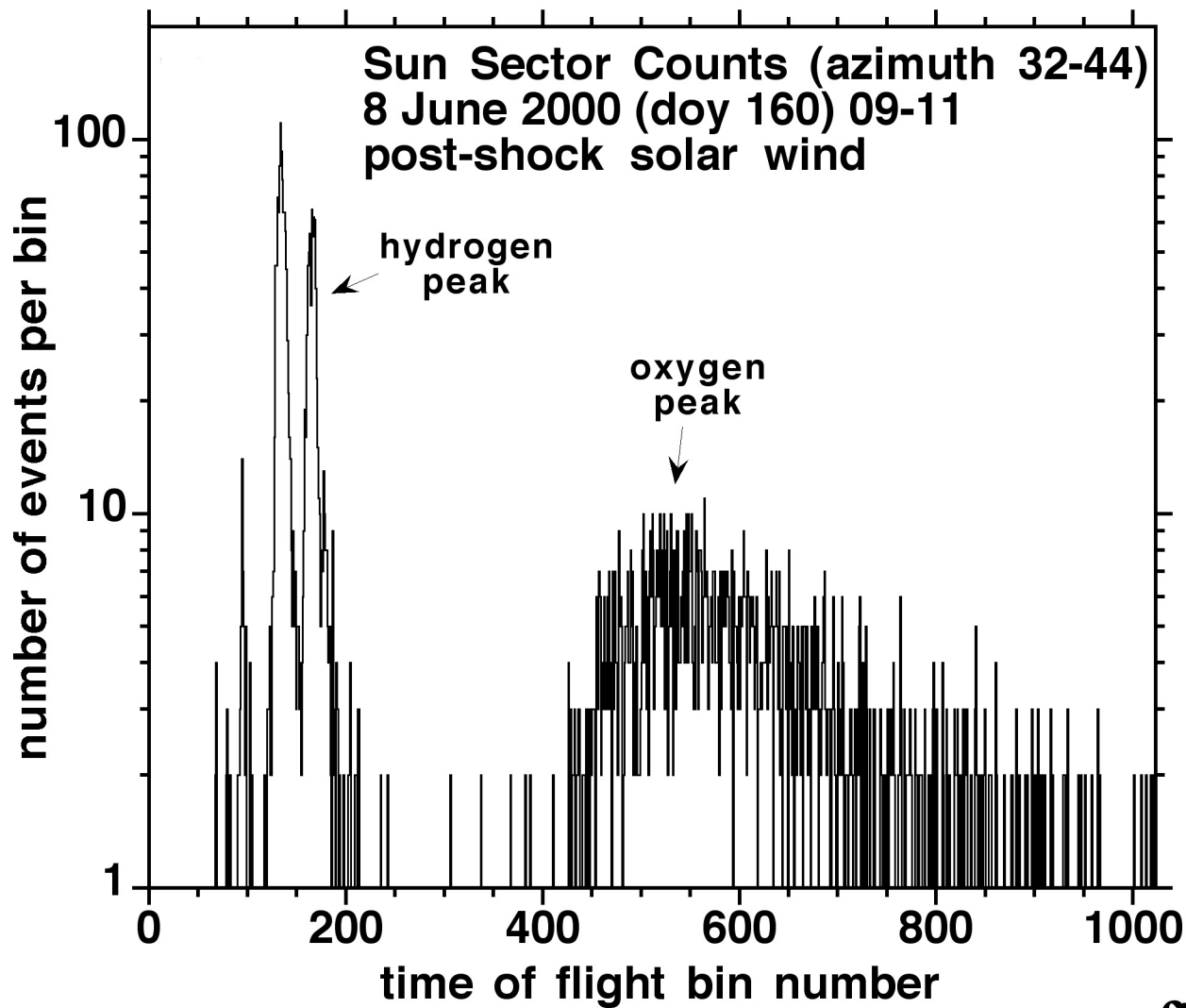


figure 5

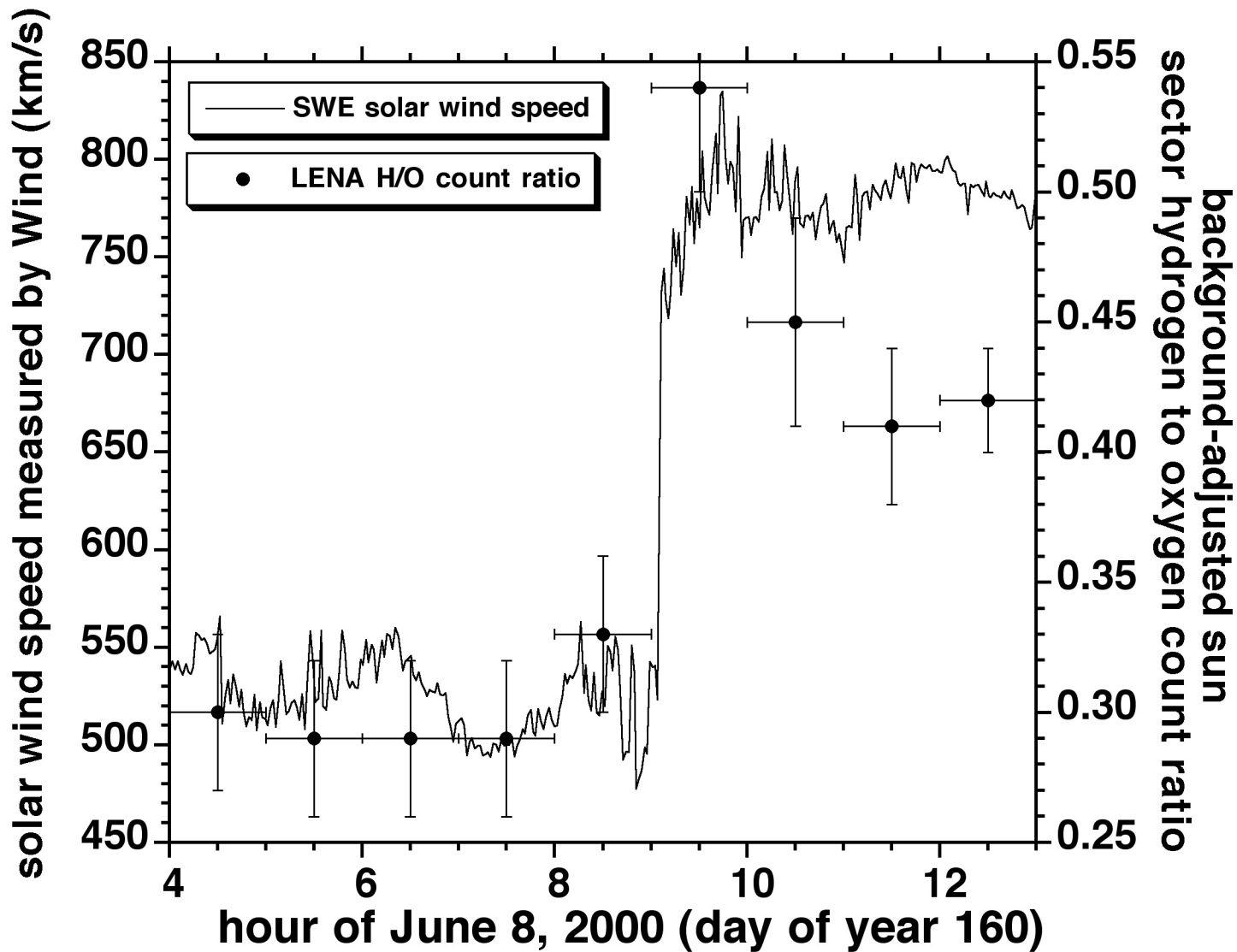


figure 6